Source parameters of a M4.8 and its accompanying repeating earthquakes off Kamaishi, NE Japan: Implications for the hierarchical structure of asperities and earthquake cycle

Naoki Uchida,[1] Toru Matsuzawa,[1] William L. Ellsworth,[2] Kazutoshi Imanishi,[3] Tomomi Okada,[1] and Akira Hasegawa[1]

Received 9 July 2007; revised 8 September 2007; accepted 25 September 2007; published 31 October 2007.

[1] We determine the source parameters of a M4.9 ± 0.1 'characteristic earthquake' sequence and its accompanying microearthquakes at ~50 km depth on the subduction plate boundary offshore of Kamaishi, NE Japan. The microearthquakes tend to occur more frequently in the latter half of the recurrence intervals of the M4.9 ± 0.1 events. Our results show that the microearthquakes are repeating events and they are located not only around but also within the slip area for the 2001 M4.8 event. From the hierarchical structure of slip areas and smaller stress drops for the microearthquakes compared to the M4.8 event, we infer the small repeating earthquakes rupture relatively weak patches in and around the slip area for the M4.8 event and their activity reflects a stress concentration process and/or change in frictional property (healing) at the area. We also infer the patches for the M4.9 ± 0.1 and other repeating earthquakes undergo aseismic slip during their interseismic period. **Citation:** Uchida, N., T. Matsuzawa, W. L. Ellsworth, K. Imanishi, T. Okada, and A. Hasegawa (2007), Source parameters of a M4.8 and its accompanying repeating earthquakes off Kamaishi, NE Japan: Implications for the hierarchical structure of asperities and earthquake cycle, *Geophys. Res. Lett.*, *34*, L20313, doi:10.1029/2007GL031263.

1. Introduction

[2] The 'characteristic earthquake' sequence off Kamaishi, NE Japan includes nine recurrences of a M4.9 ± 0.1 between 1957 and 2001 (Figure 1a, hereinafter we refer to them as M~4.9 events). *Matsuzawa et al.* [2002] discovered the sequence and suggested that these events ruptured the same patch (asperity) on the plate boundary based on their focal mechanisms and waveform similarity. *Okada et al.* [2003] estimated the slip areas for the latest two events from waveform inversion and confirmed the co-location of the two events.

[3] These studies together with analyses of other small repeating earthquake [*Uchida et al.*, 2003] and GPS data [*Nishimura et al.*, 2004; *Suwa et al.*, 2006] suggest that the earthquake cluster is isolated from other earthquakes on the plate interface and that fault creep is dominant mode of fault slip in the region surrounding the cluster. The almost constant recurrence interval (5.52 ± 0.68 years) for the sequence is attributed to a stable creep with minor fluctuation around the event [*Uchida et al.*, 2005]. Statistical analysis of the intervals suggest that the next event will occur in the near future (May 2007 ± 21month, *Matsuzawa et al.* [2002]).

[4] The earthquake cluster contains earthquakes with similar waveforms and the microearthquake activity within the cluster evolves from a low rate during the first half of the earthquake cycle to become more active during its latter half (Figure 1). The variation of microearthquake activity is probably directly related to the earthquake cycle of the M~4.9 events. Therefore, the earthquake cluster provides an excellent opportunity to study the processes during earthquake cycles.

[5] In this study, we determine high precision relative locations, source dimensions and stress drops for the earthquakes in the cluster using waveform methods to investigate slip processes that occur during the earthquake cycle of the M~4.9 events.

2. Method

2.1. Earthquake Relocation by Double-Difference Method

[6] We analyzed 25 earthquakes of M2.4 to 4.8 for the period from 1995 to 2006 in the off-Kamaishi earthquake cluster by using waveform data from the microearthquake observation network of Tohoku University (squares in the right bottom inset of Figure 1b). Most of seismometers are of 1 Hz velocity type and sampling frequency is 100 Hz.

[7] We relocated the earthquakes using waveform-based double-difference (DD) method [*Waldhauser and Ellsworth*, 2000]. We measured travel time differences using the cross spectral method of *Poupinet et al.* [1984] for both P and S waves. The time window was set to be 3.5 seconds starting 1 second before the onset of each wave and delay times were estimated from the phases of cross spectra in a frequency band of 1–10 Hz with squared coherency of greater than 0.8.

[8] We successfully obtained 13,175 and 6,695 differential travel time measurements for P and S phases, respectively, as input to the DD algorithm. Note that the 'hypocenter' estimated from correlation data is not the rupture initiation point but corresponds to the 'centroid' of the slip distribution. Therefore we refer to the relocated 'hypocenters' as 'centriods' hereafter.

[1]Research Center for Prediction of Earthquakes and Volcanic Eruptions, Tohoku University, Sendai, Japan.
[2]U.S. Geological Survey, Menlo Park, California, USA.
[3]Geological Survey of Japan, National Institute of Advanced Industrial Science and Technology, Tsukuba, Japan.

0094-8276/07/2007GL031263$05.00

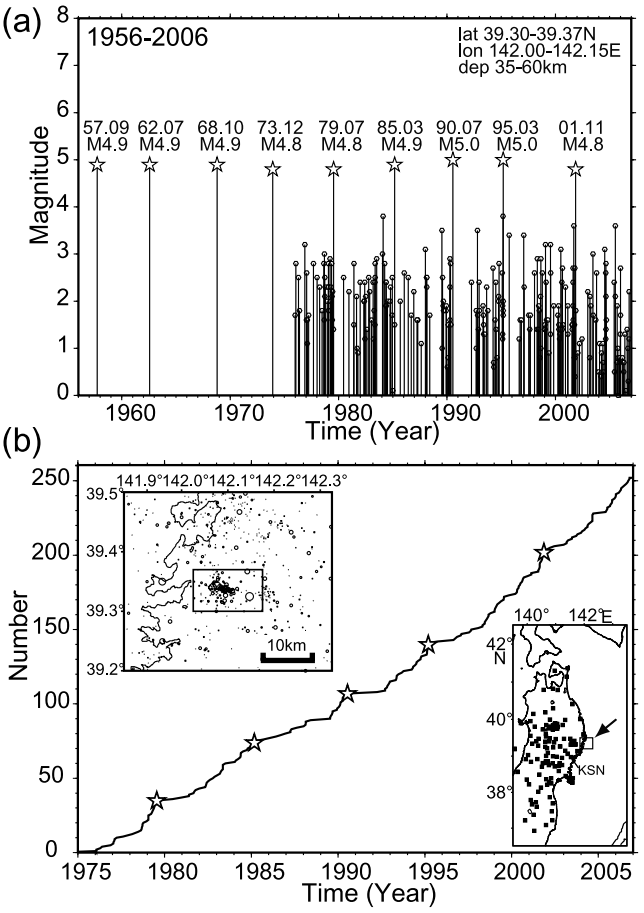

Figure 1. Seismic activity in the off-Kamaishi earthquake cluster. The data for the M4.9 ± 0.1 sequence are from *Matsuzawa et al.* [2002] and the data for other earthquakes are from the earthquake catalog of Tohoku University (1976–March 2003) and the Japan Meteorological Agency (JMA) (April 2003–2006). (a) Magnitude-time diagram of the earthquake cluster from 1956 to 2006. Magnitudes are sourced from JMA's catalogue. (Note that JMA has recently revised the catalogue and the present magnitudes are slightly different from those in the previous studies. JMA reports both displacement and velocity magnitudes for the large events and we show the displacement magnitudes for events larger than M4.5 in this study just for the convenience in the size comparison.) (b) Cumulative number of earthquakes in the earthquake cluster. Bottom right inset shows the location of the cluster (rectangle) and seismic stations (black squares). Top left inset shows the earthquake distribution in the rectangle of the bottom right inset for the period from 1976 to 2006. Earthquakes within the rectangle in the left top inset were used in the present study.

2.2. Estimation of Source Size and Stress Drop From Spectral Ratio

[9] To estimate source sizes and stress drops of the earthquakes, we estimated corner frequencies and seismic moments from their waveform spectra. We calculated Fourier amplitude spectra for P and S waves using tapered 1.0 s and 2.0 s time windows, respectively. The spectra were then resampled at equal intervals in log frequency at $\Delta\log f = 0.025$, and smoothed with running average of length $\Delta\log f = 0.2$. Spectral ratio for a pair of earthquakes recorded at the same station was calculated to eliminate path-dependent effect [*Frankel and Wennerberg*, 1989].

[10] For a robust measurement of the spectral ratios, we utilized stacking of spectral ratios (multi window spectral ratio (MWSR) method of *Imanishi and Ellsworth* [2006]). We use three windows, overlapping by half their duration, for three components at eight stations (Figure 2a). All of the spectral ratios for the same event pair were stacked if they have sufficient S/N ratio (>3). A maximum of 72 spectral ratios were stacked for a pair of earthquakes. A separate analysis is preformed for P and S waves. An example of stacked spectral ratios is shown in Figure 2b (red bold line) together with individual spectral ratios (black lines). The fluctuations in the spectral ratios have been successfully suppressed by the procedure (Figure 2b).

[11] Corner frequencies and seismic moments for the 25 events were estimated simultaneously using the multiple-empirical Green's function (MEGF) method [*Ide et al.*, 2003]. We use omega square source model spectrums proposed by *Boatwright* [1978] to model the stacked spectral ratio. We used frequency band of 1–30 Hz (60 data point for each spectral ratio) for 297 and 296 event pairs (thus total numbers of equations are 17,820 and 17,760) for P and S waves, respectively. In the inversion, we fixed the seismic moment of the 2001 M4.8 event to be 1.12×10^{16} Nm as estimated by *Okada et al.* [2003] because we need one constraint to estimate absolute scalar moments of each event.

[12] Figure 2c shows the obtained corner frequencies for P (fp) and S (fs) waves. Red circle shows result for each earthquake. The fp/fs ratios are almost constant for all earthquakes showing the reliability of the independent fp and fs estimation. The least-squares fitted line (dashed line) that passes through the origin of coordinates shows an inclination of 1.33. This value is comparable to the theoretical ratio of P to S wave corner frequencies (1.26–1.43 for the rupture velocity of $0.5–0.9\beta$, where β is a velocity of the S wave) expected from the model of *Sato and Hirasawa* [1973].

[13] Finally, we estimated the source radius (r) from the corner frequency (f_0) using the circular crack model of *Sato and Hirasawa* [1973]:

$$r = Cv/2\pi f_0, \tag{1}$$

where v is phase velocity (7.8 km for P and 4.4 km for S wave) and C is a constant. We assume C to be 1.5 for P and 1.9 for S waves. The static stress drop ($\Delta\sigma$) was then calculated by using the formula of *Eshelby* [1957]:

$$\Delta\sigma = (7/16)\left(M_0/r^3\right), \tag{2}$$

where M_0 is seismic moment. As the final source radiuses and stress drops, we adopted weighted average of the values estimated from P and S waves, where the weights were set to be proportional to the number of spectral ratios in the stack.

3. Results

3.1. Earthquake Distribution

[14] The results are summarized in Figure 3a, where the centers of circles indicate the earthquake centroid locations

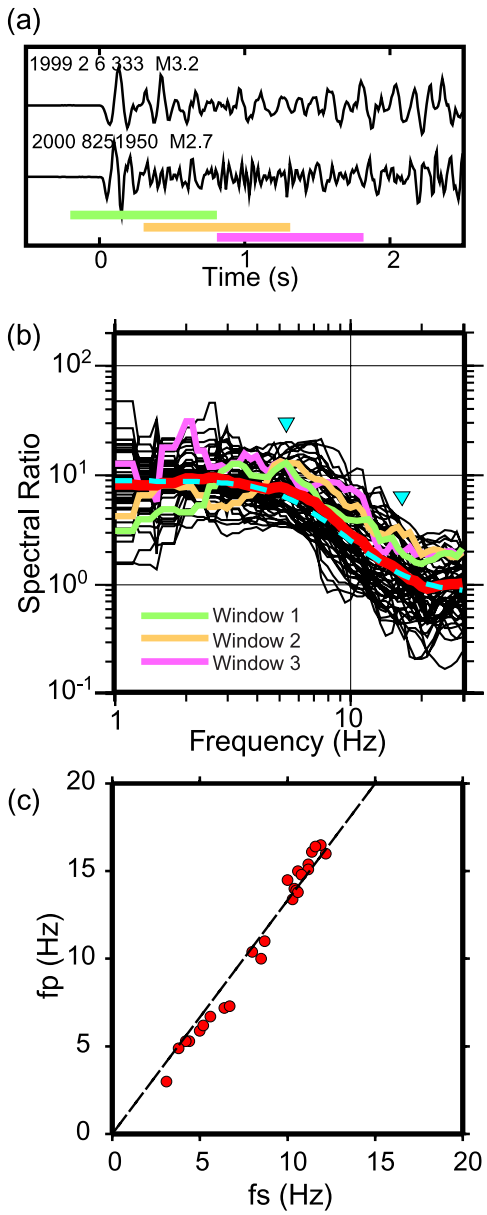

Figure 2. Example of spectral ratio analyses and the resulting corner frequencies. (a) Vertical component waveforms at KSN station (Figure 1b). The earthquakes shown in the upper and lower seismogram are members of the cluster A and C in Figure 3, respectively. (b) Spectral ratios for various time windows, components, and stations (black thin lines) and stacked spectral ratio (red bold line) for the event pair shown in Figure 2a. Colored spectral ratios are derived from the time windows indicated by the same color bars below the seismograms in Figure 2a. Theoretical spectral ratio (dashed blue line) and corner frequencies (blue inverted triangle) are also shown for the event pair calculated from an omega square model. (c) Comparison of corner frequencies for P wave (fp) and S waves (fs). Each red dot shows the corner frequency for each earthquake. Dashed line denotes the least-squares fit for the dots (fp = 1.33 fs).

(see auxiliary material for the list of parameters).[1] The location errors shown by bars are typically 20m which was estimated from the residuals of DD data. The boot-strap method by the same procedure by *Waldhauser and Ellsworth* [2000] also shows errors as small as ~30 m. The centroids are aligned in the east-west direction and on a westwardly dipping plane (striking 180 degrees, dipping 38 degrees) that may delineate the subduction interface (see east-west cross-section shown in the inset of Figure 3a).

[15] The result shows that the microearthquakes are located mainly in three clusters (A, B1 + B2, C) and that the centroid of the 2001 M4.8 event is located very close to those of the earthquakes in the clusters B1 and B2. Note that the location of the centroid of the M4.8 event relative to the other events was determined accurately by our analysis. The location of the hypocenter (black diamond) estimated by *Okada et al.* [2003] falls within clusters B1 and B2.

3.2. Source Size

[16] Rupture dimensions determined from the spectral ratios are projected onto the 38 degree west-dipping plane in Figure 3a. The rupture dimension errors estimated by the boot-strap method using residuals of spectral ratios are typically 6% of their diameters. Although the slip areas of the earthquakes are likely more complex, we consider that these circles centered at the centroids are a good first approximation. Considering the source sizes and location uncertainty, it is certain that the microearthquakes in each cluster are co-located with one or more other events (i.e. they are repeating earthquakes). For the 2001 M4.8 event, we estimated the diameter of the source area to be 1.1 km which is comparable to the estimation from waveform inversion (1.0–1.5 km, *Okada et al.* [2003]). The western cluster (Cluster A) which consists of relatively large (M2.9–3.8) earthquakes seems to be positioned near the edge of the source area of the 2001 M4.8 event. The eastern cluster (Cluster C) seems to be just outside the source area of the M4.8 event. The middle cluster (Cluster B) lies within the interior of the slip area for the M4.8 event.

3.3. Static Stress Drop and Earthquake Activity in Each Cluster

[17] The static stress drops are indicated by color of circles in Figure 3a. Figure 3a shows that the stress drop of the M4.8 event (39 MPa) is much higher than those of the other events (3–11 Mpa) and stress drops of the earthquakes within each cluster tend to have similar values (i.e. similar colors in Figure 3a). The errors for stress drops estimated by the boot-strap method are 4 MPa for the M4.8 event and typically 1 MPa for the other events.

[18] Magnitude-time plot of the earthquakes for the three clusters (Figure 3b) shows that the abundant earthquakes in the latter half of the earthquake cycles of the M~4.9 events (yellow stars) include members from each of the three clusters, especially for the clusters B (squares) and C (diamonds). The earthquakes at cluster B1 (green squares) occurred within 1 month after the earthquakes at cluster A (red triangles). We also point out that there always occurred earthquakes at cluster A within three month before the M~4.9 events, although the activity in

[1] Auxiliary materials are available at ftp://ftp.agu.org/apend/gl/2007gl031263.

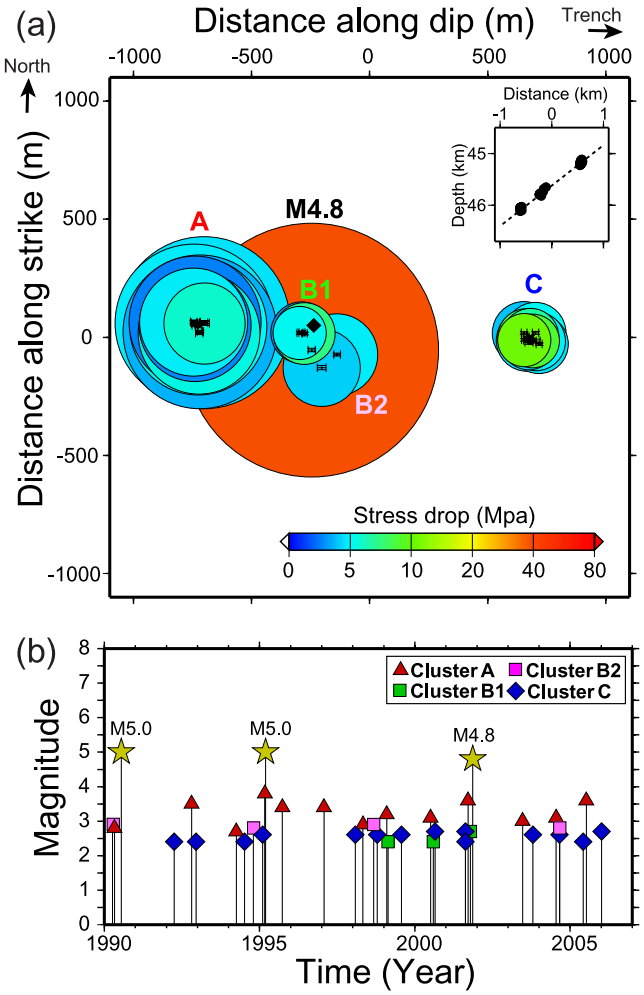

Figure 3. (a) Location, rupture area, and static stress drop for the earthquake cluster projected on the 38 degree westward dipping plane. See auxiliary material for the list of parameters. Circles denote the source sizes and the center of the circle is the centroid of each earthquake. Small bars denote 2σ centroid location errors. Color shows stress drops. Inset shows east-west cross-section of the centriods (black dots). (b) Magnitude-time diagram for the earthquake clusters A, B1, B2, and C defined in Figure 3a. Earthquakes with magnitude 2.4 or larger for the time range before the analyses period (1990 to March 1995) are also plotted. These events were grouped based on the waveform similarity.

the cluster A seems to be more independent of the M∼4.9 events than that in the clusters B and C.

[19] The cumulative slip for the period between 1995 and 2001 events (interseismic period of the M∼4.9 events) are estimated to be 10–17, 3.0–4.7, 1.2–2.0 and 6.9–11 cm for the cluster A, B1, B2, and C, respectively, whereas the slip for the 2001 event is 25–41 cm (Here, we used radius and seismic moment of each event and assumed the rigidity as $3.0–5.0 \times 10^{10}$ N/m^2).

4. Discussion

4.1. Seismicity Rate Change During Earthquake Cycle

[20] Changes in the rate of earthquakes over the seismic cycle have been observed in some case studies [e.g., *Mogi*, 1981; *Ellsworth et al.*, 1981]. The off-Kamaishi M4.9 ± 0.1 'characteristic earthquake' sequence provides an excellent opportunity to investigate earthquake rate systematics.

[21] The results obtained in this study show that the increasing seismicity or frequent occurrence of earthquakes in the latter half of the recurrence intervals of the M∼4.9 events was mainly due to the earthquake activity close to or within the slip area (∼1 km × 1 km) of the 2001 M4.8 event. Most of them are located in three patches and have smaller stress drops than the M4.8 event. The successive occurrences of earthquakes for clusters A–B and A–M∼4.9 suggest some interaction between these events.

[22] From these observations we consider three possibilities for the cause of the higher rate of microearthquakes in the latter half of the recurrence intervals of the M∼4.9 events: (1) Recovery of the stress shadow from the previous M∼4.9 event due to creep in the region surrounding the sources (Note that the small asperities close to the M∼4.9 experienced slip larger than usual when the M∼4.9 event occurred); (2) Delayed relocking of the source regions of the repeating microearthquakes due to a slow rate of fault healing (change in frictional properties); and (3) Unlocking of portions of the coseismic slip area of the M∼4.9 events after a critical stress threshold was reached loads the source areas of the smaller repeating events. Although it is difficult to know which process dominates in the off–Kamaishi cluster, we think models (1) and/or (3) are plausible for the cluster B as we will discuss in the next section, while (2) is plausible for the cluster C because it is relatively far from the M4.8.

4.2. Source Property and Coupling Coefficient of Repeating Earthquakes

[23] The source properties of small repeating earthquakes have been investigated in many studies. *Rubin et al.* [1999], *Schaff et al.* [2002], *Waldhauser and Ellsworth* [2000] and *Waldhauser et al.* [2004] have shown that the small repeating earthquakes on the Hayward, San Andreas and Calaveras faults commonly form horizontal streaks parallel to the slip vector. This suggests rheological transitions within the fault zone and/or geometrical complexity of the fault that concentrate stress in the boundary between locked and creeping areas evolve with increasing fault slip. The centroids of the off–Kamaishi cluster similarly align with the slip vector between the Pacific plate and NE Honshu, suggesting a similar evolutionary mechanism may be operating there.

[24] Our results show that the recurrence cycle for the M∼4.9 events is considerably more complex than the simple reaccumulation of strain energy on a locked patch: The coseismic slip area for the 2001 M4.8 event includes repeating events deep within its interior, near its centroid or hypocenter (cluster B1 and B2). We note that the recurrence properties of M∼4.9 events are simpler in spite of the complex internal structure of the asperity. This observation is important to model earthquake cycle including larger earthquakes and also to investigate behavior of general complex systems with self–similar structure.

[25] These small events also suggest the occurrence of aseismic slip inside the rupture area of the M4.8 event because they must be repeatedly reloaded during the repose of the M∼4.9 events. The occurrence of aseismic slip

during the interseismic period was proposed by *Beeler et al.* [2001] to explain the relationship between recurrence time and seismic moment for small repeating earthquakes at Parkfield [*Nadeau and Johnson*, 1998]. The slip amount for the 2001 M4.8 event (25–41 cm) also suggests the occurrence of aseismic slip during the interseismic period because the slip amount is smaller than the expected slip deficit (57 cm) estimated from plate convergence rate (8.5 cm/year) and time period (6.7 years) after the 1995 event. *Okada et al.*'s [2003] slip distribution also show that the slip amount (16–26 cm at the maximum) is smaller than the slip deficit. The cumulative seismic slip for cluster C (6.9–11 cm) for the period between 1995 and 2001 event also suggests the existence of the aseismic slip during the interseismic period.

5. Conclusions

[26] We have estimated source properties for small earthquakes that show prominent activity in the latter half of the recurrence intervals of the M4.9 ± 0.1 'characteristic earthquake' sequence off Kamaishi, NE Japan. We found the earthquakes are located very close to the source area of the 2001 M4.8 event (within 1 km from centroid of the 2001 M4.8 event and near the edge or inside the slip area), and most of the events within the clusters were co–located, forming their own 'characteristic earthquake' sets. We also found the smaller events tend to have small stress drops (2.6–10.8 MPa) compared to the M4.8 event (39 MPa).

[27] The present observation suggests the small earthquakes occur on relatively weak patches in and around the source area for the M∼4.9 event. The systematic increase in the rate of their activity during the seismic cycle probably reflects the temporal variation in stress or frictional properties in and around the M∼4.9 events.

[28] There are earthquakes within the slip area of the M4.8 event and the seismic slip of the M4.8 event was less than the slip expected from the plate convergence rate. These results imply the source region of the small repeating earthquake undergoes aseismic slip in their interseismic period.

[29] **Acknowledgments.** We thank T. Yamashita for providing programs for stress drop data analysis, T. Igarashi, and S. Kirby for fruitful discussion, J. Hardebeck and N. Beeler for comments that improved the manuscript, and Y. Iio and T. Hori for constructive reviews. This work was partially supported by KAKENHI 19740264 and the 21st Century Center of Excellence program, 'Advanced Science and Technology Center for the Dynamic Earth' at Tohoku University.

References

Beeler, N. M., D. L. Lockner, and S. H. Hickman (2001), A simple stick-slip and creep-slip model for repeating earthquakes and its implication for microearthquakes at Parkfield, *Bull. Seismol. Soc. Am.*, *91*, 1797–1804.

Boatwright, J. (1978), Detailed spectral analysis of two small New York State earthquakes, *Bull. Seismol. Soc. Am.*, *68*, 1117–1131.

Ellsworth, W. L., A. G. Lindh, W. H. Prescott, and D. G. Herd (1981), The 1906 San Francisco earthquake and the seismic cycle, in *Earthquake Prediction: An International Review*, *Maurice Ewing Ser.*, vol. 4, edited by D. W. Simpson and P. G. Richards, pp. 126–140, AGU, Washington, D. C.

Eshelby, J. D. (1957), The determination of the elastic field of an ellipsoidal inclusion and related problems, *Proc. R. Soc. London, Ser. A*, *241*, 376–396.

Frankel, A., and L. Wennerberg (1989), Microearthquake spectra from the Anza, California, seismic network: Site response and source scaling, *Bull. Seismol. Soc. Am.*, *79*, 581–609.

Ide, S., G. C. Beroza, S. G. Prejean, and W. L. Ellsworth (2003), Apparent break in earthquake scaling due to path and site effects on deep borehole recordings, *J. Geophys. Res.*, *108*(B5), 2271, doi:10.1029/2001JB001617.

Imanishi, K., and W. L. Ellsworth (2006), Source scaling relationships of microearthquakes at Parkfield, CA, determined using the SAFOD Pilot Hole Seismic Array, in *Earthquakes: Radiated Energy and the Physics of Earthquake Faulting*, *Geophys. Monogr. Ser.*, vol. 170, edited by R. Abercrombie et al., pp. 81–90, AGU, Washington, D. C.

Matsuzawa, T., T. Igarashi, and A. Hasegawa (2002), Characteristic small-earthquake sequence off Sanriku, northeastern Honshu, Japan, *Geophys. Res. Lett.*, *29*(11), 1543, doi:10.1029/2001GL014632.

Mogi, K. (1981), Seismicity in western Japan and long-term earthquake forecasting, in *Earthquake Prediction: An International Review*, *Maurice Ewing Ser.*, vol. 4, edited by D. W. Simpson and P. G. Richards, pp. 43–51, AGU, Washington, D. C.

Nadeau, R. M., and L. R. Johnson (1998), Seismological studies at Parkfield VI: Moment release rates and estimates of source parameters for small repeating earthquakes, *Bull. Seismol. Soc. Am.*, *88*, 790–814.

Nishimura, T., T. Hirasawa, S. Miyazaki, T. Sagiya, T. Tada, S. Miura, and K. Tanaka (2004), Temporal change of interplate coupling in northeastern Japan during 1995–2002 estimated from continuous GPS observations, *Geophys. J. Int.*, *157*, 901–916.

Okada, T., T. Matsuzawa, and A. Hasegawa (2003), Comparison of source areas of M4.8 ± 0.1 earthquakes off Kamaishi, NE Japan-Are asperities persistent features?, *Earth Planet. Sci. Lett.*, *213*, 361–374.

Poupinet, G., W. L. Ellsworth, and J. Frechet (1984), Monitoring velocity variations in the crust using earthquake doublets: An application to the Calaveras Fault, California, *J. Geophys. Res.*, *89*, 5719–5731.

Rubin, A. M., D. Gillard, and J.-L. Got (1999), Streaks of microearthquakes along creeping faults, *Nature*, *400*, 635–641.

Sato, T., and T. Hirasawa (1973), Body wave spectra from propagating shear cracks, *J. Phys. Earth*, *21*, 415–431.

Schaff, D. P., G. H. R. Bokelmann, G. C. Beroza, F. Waldhauser, and W. L. Ellsworth (2002), High resolution image of Calaveras Fault seismicity, *J. Geophys. Res.*, *107*(B9), 2186, doi:10.1029/2001JB000633.

Suwa, Y., S. Miura, A. Hasegawa, T. Sato, and K. Tachibana (2006), Interplate coupling beneath NE Japan inferred from three-dimensional displacement field, *J. Geophys. Res.*, *111*, B04402, doi:10.1029/2004JB003203.

Uchida, N., T. Matsuzawa, T. Igarashi, and A. Hasegawa (2003), Interplate quasi-static slip off Sanriku, NE Japan, estimated from repeating earthquakes, *Geophys. Res. Lett.*, *30*(15), 1801, doi:10.1029/2003GL017452.

Uchida, N., T. Matsuzawa, A. Hasegawa, and T. Igarashi (2005), Recurrence intervals of characteristic M4.8 ± 0.1 earthquakes off Kamaishi, NE Japan-Comparison with creep rate estimated from small repeating earthquake data, *Earth Planet. Sci. Lett.*, *233*, 155–165.

Waldhauser, F., and W. L. Ellsworth (2000), A double-difference earthquake location algorithm: Method and application to the Northern Hayward fault, California, *Bull. Seismol. Soc. Am.*, *90*, 1353–1368.

Waldhauser, F., W. L. Ellsworth, D. P. Schaff, and A. Cole (2004), Streaks, multiplets, and holes: High-resolution spatio-temporal behavior of Parkfield seismicity, *Geophys. Res. Lett.*, *31*, L18608, doi:10.1029/2004GL020649.

W. L. Ellsworth, U.S. Geological Survey, Mail Stop 977, 345 Middlefield Road, Menlo Park, CA 94025, USA.

A. Hasegawa, T. Matsuzawa, T. Okada, and N. Uchida, Research Center for Prediction of Earthquakes and Volcanic Eruptions, Tohoku University, Aramaki Aza Aoba, Aoba-ku, Sendai 980-8578, Japan. (uchida@aob.geophys.tohoku.ac.jp)

K. Imanishi, Geological Survey of Japan, AIST, Tsukuba Central 7 1-1, Higashi 1, Tsukuba, Ibaraki-ken 305-8567, Japan.